Наносистеми, наноматеріали, нанотехнології
Nanosystems, Nanomaterials, Nanotechnologies
2009, т. 7, № 3, сс. 793–801

PACS numbers: 05.45.Df, 41.20.Jb, 42.25.-p, 61.43.Hv, 68.35.Ct, 78.68.+m, 81.70.Fy

Features of Light Scattering by Surface Fractal Structures

O. Yu. Semchuk, D. L. Vodopianov, and L. Yu. Kunitska

O. O. Chuiko Institute of Surface Chemistry, N.A.S. of Ukraine,
17 General Naumov,
03164 Kyyiv, Ukraine

The average coefficient of light scattering by surface fractal structures is calculated within the scope of the Kirchhoff's method. Two-dimensional band-limited Weierstrass function is used to simulate a scattering surface. On the basis of numerical calculations of average scattering coefficient, the scattering indicatrixes for various surfaces and incidence angles are calculated. The analysis of the indicatrixes leads to the following conclusions: the scattering is symmetric about the incidence plane; with the increase of surface calibration degree, the scattering pattern becomes more complicated; the greatest intensity of the scattered wave is observed along the mirror direction; there are other directions, in which the intensity bursts are observed.

В рамках Кирхгоффової методи розраховано середній коефіцієнт розсіяння світла поверхневими фрактальними структурами. Для моделювання розсіювальної поверхні використовувалася двовимірна, обмежена смугою Вейєрштрассова функція. Виконано чисельні розрахунки середнього коефіцієнта розсіяння та побудовано індикатриси розсіяння для різних типів поверхонь та кутів падіння. Аналіза індикатрис розсіяння призводить до наступних висновків: розсіяння є симетричним відносно площини падіння; зі збільшенням ступеня калібрування поверхні картина розсіяння ускладнюється; найбільша інтенсивність розсіяної хвилі спостерігається в дзеркальному напрямку і, крім того, існують напрямки, в яких спостерігаються сплески інтенсивности.

В рамках метода Кирхгофа рассчитан средний коэффициент рассеяния света поверхностными фрактальными структурами. Для моделирования рассеивающей поверхности использовалась двумерная, ограниченная полосой функция Вейерштрасса. Произведены численные расчеты среднего коэффициента рассеяния и построены индикатрисы рассеяния для различных поверхностей и углов падения. Анализ индикатрис рассеяния приводит к следующим заключениям: рассеяние является симметричным относительно плоскости падения; с увеличением степени калибровки поверхности картина рассеяния усложняется; наибольшая интенсивность

рассеянной волны наблюдается в зеркальном направлении и, кроме того, существуют другие направления, в которых наблюдаются всплески интенсивности.

Key words: fractal surface, light, wave, indicatrixe, rough surface.

(Received 20 October, 2008)

1. INTRODUCTION

Accurate measurement of surface roughness of machined work pieces is of fundamental importance particularly in the precision engineering and manufacturing industry. This is caused by the more stringent demands on material quality as well as the miniaturization of product components in these industries [1–3]. For instance, in the disk drive industry, to maintain the quality of the electrical components mounted on an optical disk, the surface roughness of the disk must be accurately measured and controlled. Hence, the surface finish, normally expressed in terms of surface roughness, is a critical parameter used for the acceptance or rejection of a product.

Surface roughness is usually determined by a mechanical stylus profilometre. However, the stylus technique has certain limitations: the mechanical contact between the stylus and the object can cause deformations or damage of the specimen surface and it is a point wise and time-consuming measurement method. Hence, a noncontact and faster optical method would be attractive. Different optical noncontact methods for surface roughness measuring were developed. They are based on reflected light detection, focus error detection, laser scattering, speckle and interference measurements [4–10]. Some of them have a good resolution and are applied in some sectors where mechanical measurement methods previously enjoyed clear predominance. Among these methods, the light scattering method [11] is a noncontact area-averaging technique and is potentially faster for surface inspection than other profiling techniques, particularly, the traditional stylus technique. Other commercially available products such as the scanning tunnelling microscope (STM), the atomic force microscope (AFM) and subwavelength photoresist gratings [12–15], which are pointwise techniques, are used mainly for optically smooth surfaces with roughness in the nanometre range.

In this paper, the average coefficient of light scattering by surface fractal structures was calculated in the frameworks of the Kirchhoff's method (scalar model). A normalized band-limited Weierstrass function was used to simulate $2D$ fractal rough surfaces. On the basis of numerical calculation of average scattering coefficient, the scattering indicatrixes for various surfaces and incidence angles were calculated. The

analysis of the indicatrixes leads us to the following conclusions: the scattering is symmetric about the incidence plane; with the increase of surface calibration degree, the scattering pattern becomes more complicated; the greatest intensity of the scattered wave is observed along the mirror direction; there are other directions, in which the intensity bursts are observed.

2. FRACTAL MODEL FOR TWO-DIMENSIONAL ROUGH SURFACES

The following form of the modified two-dimensional band-limited Weierstrass function is proposed:

$$z(x,y) = c_w \sum_{n=0}^{N-1} \sum_{m=1}^{M} q^{(D-3)n} \sin\left\{ Kq^n \left[x\cos\frac{2\pi m}{M} + y\sin\frac{2\pi m}{m} \right] + \varphi_{nm} \right\}, \quad (1)$$

where c_w is a constant, which ensures that $W(x, y)$ has a unit perturbation amplitude; q $(q > 1)$ is the fundamental spatial frequency; D $(2 < D < 3)$ is the fractal dimension; K is the fundamental wavenumber; N and M are number of tones, and φ_{nm} is a phase term that has a uniform distribution over the interval $[-\pi, \pi]$.

The above function is a combination of both deterministic periodic and random structures. This function is anisotropic in two directions if M and N are not too large. It has a large derivative and is self-similar. It is a multiscale surface, which has same roughness down to some fine scales. Since natural surfaces are generally neither purely random nor purely periodic and often anisotropic, the function proposed above is a good candidate to model natural surfaces.

The phases φ_{nm} can be chosen determinedly or casually, obtaining accordingly determine or stochastic function $z(x, y)$. We shall further consider φ_{nm} as casual values, which are regularly distributed on an interval $[-\pi, \pi]$. For each particular choice of numerical value of all $N \times M$ phases, φ_{nm} (for example, by means of the random numbers generator), we obtain particular (with the meanings of parameters c_w, q, K, D, N, M chosen in advance) realization of function $z(x, y)$. Every possible realization of function $z(x, y)$ forms an ensemble of surfaces.

Deviation of points of a rough surface from a basic plane is proportional to c_w; therefore, this parameter is connected with the height of surface structure irregularities. Further, a rough surface is determined, specifying root-mean-square height of its structure σ, which is determined by such expression:

$$\sigma \equiv \sqrt{\langle h^2 \rangle}, \quad (2)$$

where $h = z(x, y)$, $\langle \ldots \rangle = \prod_{n=0}^{N-1} \prod_{m=1}^{M} \int_{-\pi}^{\pi} \frac{d\varphi_{nm}}{2\pi} (\ldots)$ —averaging over ensemble of

surfaces.

The relationship between c_w and σ can be established by direct calculation of integrals:

$$\sigma = \left[\prod_{n=0}^{N-1} \prod_{m=1}^{M} \int_{-\pi}^{\pi} \frac{d\varphi_{nm}}{2\pi} z^2(x, y) \right]^{\frac{1}{2}} = c_w \left[\frac{M\left(1 - q^{2N(D-3)}\right)}{2\left(1 - q^{2(D-3)}\right)} \right]^{\frac{1}{2}}. \quad (3)$$

So, the rough surface in our model is described by function of six parameters: c_w (or σ), q, K, D, N, M. The influence of different parameters on a kind of a surface can be investigated both analytically and studying structures of surfaces constructed by results of numerical calculations of Weierstrass function. Thus, it was found out that:

the wave number K determines the wavelength of the basic harmonic of the surface;

the numbers, N, M, D, and q, determine a degree of surface calibration at the expense of imposing of additional harmonics on the basic wave, and N and M determine the number of harmonics, which are imposed;

D determines amplitude of harmonics;

q determines both amplitude and frequency of harmonics.

Let us note that, with increase of N, M, D, and q, the spatial uniformity of the surface on a large scale is also increased.

3. LIGHT SCATTERING ON SURFACE FRACTAL STRUCTURES

Experiment diagram of light scattering is presented in Fig. 1.

The initial light wave falls on a rough surface S under angle θ_1 and is scattered in all directions. The scattering wave is registered by the de-

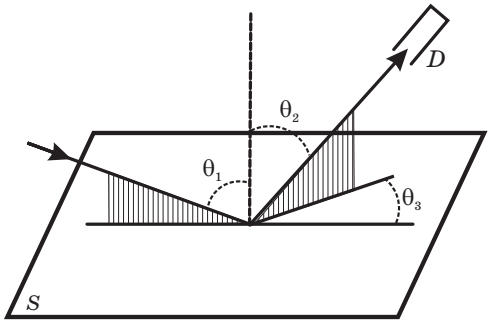

Fig. 1. Experiment diagram for light scattering by fractal surface; S is a scattering surface; D—detector, θ_1 is an incidence angle; θ_2 is a polar angle; θ_3 is an azimuth angle.

tector D in the direction, which is characterized by a polar angle θ_2 and an azimuthal angle θ_3. The intensity of light I_s scattered in (θ_2, θ_3) direction is measured. Our goal is construction of indicatrix of electromagnetic wave scattering by a fractal surface (1).

As $I_s = \mathbf{E}_s\mathbf{E}_s^*$ (where $\mathbf{E}_s$ is an electric field of the scattered wave in complex representation), the problem of I_s finding is reduced to finding of the scattered field $\mathbf{E}_s$.

We shall find the scattered field using Kirchhoff's method [16], and considering complexity of a problem, we shall take advantage of simpler scalar variant of the theory, according to which the electromagnetic field is described by scalar variable. Thus, we lose an opportunity to analyze polarizing effects.

The base formula of Kirchhoff's method makes it possible to find the scattered field under such conditions:

the incident wave is monochromatic and plane;

a scattering surface is rough inside some rectangular ($-X < x_0 < X$, $-Y < y_0 < Y$) and smooth outside of its boundaries;

the size of the rough site is significantly greater than length of incident wave;

all points of the surface have finite gradient;

the reflection coefficient is identical for all points of the surface;

the scattered field is observed in a wave zone, *i.e.* well away from the scattering surface.

Under these conditions, the scattered field is given by

$$E_s(\mathbf{r}) = -ikrF\left(\theta_1, \theta_2, \theta_3\right)\frac{\exp(ikr)}{2\pi r}\int\limits_{S_0}\exp[ik\varphi(x_0, y_0)]dx_0dy_0 + E_e(\mathbf{r}), \quad (4)$$

where k is the wave number of incident wave; $F(\theta_1, \theta_2, \theta_3) = -\frac{R}{2C}\left(A^2 + B^2 + C^2\right)$ is the angle factor; $A = \sin\theta_1 - \sin\theta_2\cos\theta_3$; $B = -\sin\theta_2\sin\theta_3$; $C = -\cos\theta_1 - \cos\theta_2$; R is the scattering coefficient; $\varphi(x_0, y_0) = Ax_0 + By_0 + Ch(x_0, y_0)$ is the phase function; $h(x_0, y_0) = z(x_0, y_0)$; $E_e(\mathbf{r}) = -\frac{R}{C}\frac{\exp(ikr)}{4\pi r}\left(AI_1 + BI_2\right)$,

$$I_1 = \int\limits_{-Y}^{Y}\left[e^{ik\varphi(X, y_0)} - e^{ik\varphi(-X, y_0)}\right]dy_0, \quad I_2 = \int\limits_{-X}^{X}\left[e^{ik\varphi(x_0, Y)} - e^{ik\varphi(x_0, -Y)}\right]dx_0. \quad (5)$$

After calculation of integrals (4) and (5) using formula $e^{iz\sin\phi} = \sum\limits_{l=-\infty}^{\infty} I_l\left(z\right)e^{il\phi}$, where $I_1(z)$ is the Bessel function of integer order, we obtain:

$$E_s(\mathbf{r}) = -2ikFXY\frac{\exp(ikr)}{\pi r}\sum_{l_{\{rs\}}}\left\{\left[\prod_{uv} I_{l_{uv}}(\xi_u)\right]e^{i\sum\limits_{nm} l_{nm}\varphi_{nm}}\right\}\sin c(k_c X)\sin c(k_s Y) + E_e(\mathbf{r}) \tag{6}$$

where $F = F(\theta_1, \theta_2, \theta_3)$,

$$\sum_{l_{\{rs\}}} \equiv \sum_{l_{0,1}=-\infty}^{\infty}\sum_{l_{0,2}=-\infty}^{\infty}\cdots\sum_{l_{(N-1),M=-\infty}}^{\infty}, \qquad \prod_{uv} \equiv \prod_{u=1}^{N-1}\prod_{v=0}^{M}, \qquad \sum_{nm} \equiv \sum_{n=1}^{N-1}\sum_{m=0}^{M},$$

$$\xi_u \equiv kc_w Cq^{(D-3)u}, \quad \sin cx \equiv \frac{\sin x}{x},$$

$$k_c \equiv kA + K\sum_{nm} q^n l_{nm}\cos\frac{2\pi m}{M}, \quad k_s \equiv kB + K\sum_{nm} q^n l_{nm}\sin\frac{2\pi m}{M},$$

$$E_e(\mathbf{r}) = -ikXY\frac{R}{C}\left(A^2 + B^2\right)\frac{e^{ikr}}{\pi r}\sin c\left(kAX\right)\sin c\left(kBY\right).$$

Thus, expression (6) gives the solution of the problem of finding of field scattering by a fractal surface within the frameworks of Kirchhoff's method.

Now, it is possible to calculate intensity of scattered waves using formula (4) if parameters of the scattering surface c_w (or σ), D, q, K, N, M, X, Y, ϕ_{nm}, parameter k $\left(\text{or } \lambda = \frac{2\pi}{k}\right)$ of the incident wave, and parameters θ_1, θ_2, θ_3 of geometry of experiment are known. This intensity will characterize scattering of specific realization of the surface $z(x, y)$ (with a specific set of casual phases ϕ_{nm}). For comparison of calculations with experimental data, it is necessary to operate with intensity averaged over ensemble of surfaces: $\langle I_s\rangle = \langle \mathbf{E}_s\mathbf{E}_s^*\rangle$. This intensity is proportional to intensity $I_0 = \left(\frac{2kXY\cos\theta_1}{\pi r}\right)^2$ of the wave reflected from the corresponding smooth basic surface. Therefore, for the theoretical analysis of results, it is more convenient to use averaged scattering coefficient: $\langle \rho_s\rangle = \frac{\langle I_s\rangle}{I_0}$.

After calculation of $\langle I_s\rangle$ and starting from (6), we obtain exact expression:

$$\langle \rho_s\rangle = \left[\frac{F(\theta_1, \theta_2, \theta_3)}{\cos\theta_1}\right]\sum_{l_{\{rs\}}}\left\{\prod_{uv} I_{l_{uv}}^2(\xi_u)\sin c^2(k_c X)\sin c^2(k_s Y)\right\} +$$

$$+\left[\frac{R\left(A^2+B^2\right)}{2C\cos\theta_1}\right]^2 \sin c^2\left(kAX\right)\sin c^2\left(kBY\right). \qquad (7)$$

As expression (7) consists of the infinite sum, it is inconvenient to use for numerical calculations. Essential simplification is reached in the case when $\xi_n < 1$. Using series expansion of function as follows,

$$I_\nu\left(z\right)=\left(\frac{3}{2}\right)^\nu \sum_{k=0}^{\infty}\frac{\left(-z^2/4\right)^k}{k!\,\Gamma\left(\nu+k+1\right)},$$

and rejecting terms of orders greater than ξ_n^2, we obtain the approximate expression for averaged scattering coefficient

$$\left\langle \rho_s \right\rangle \approx \left[\frac{F\left(\theta_1,\theta_2,\theta_3\right)}{\cos\theta_1}\right]^2 \left\{\left[1-\left(k\sigma C\right)^2\right]\sin c^2\left(kAX\right)\sin c^2\left(kBY\right)+\right.$$

$$+\frac{1}{2}c_f^2\sum_{nm} q^{2(D-3)n}\sin c^2\left[\left(kA+Kq^n\cos\frac{2\pi m}{M}\right)X\right]\sin c^2+$$

$$\left.+\left[\left(kB+Kq^n\sin\frac{2\pi m}{M}\right)Y\right]\right\}+$$

$$+\left[\frac{R}{2C\cos\theta_1}\left(A^2+B^2\right)\right]^2 \sin c^2\left(kAX\right)\sin c^2\left(kBY\right), \qquad (8)$$

where $c_f \equiv kc_w C = k\sigma C\left[\frac{2}{M}\frac{1-q^{2(D-3)}}{1-q^{2N(D-3)}}\right]^{\frac{1}{2}}$.

4. RESULTS OF NUMERICAL CALCULATIONS

On the basis of numerical calculations of average factor of scattering according to formula (8), we constructed the dependence of the averaged scattering coefficient $\left\langle \rho_s \right\rangle$ on θ_2 and θ_3 (scattering indicatrixes) for different types of scattering surfaces. At these calculations, we supposed that $R = 1$, and, consequently, did not consider real dependence of reflection coefficient R on the incidence wavelength, λ, and incidence angle, θ_1. The obtained results are presented in Fig. 2.

The analysis of the indicatrixes leads us to the following conclusions:
the scattering is symmetric about the incidence plane;
the greatest intensity of the scattered wave is observed along the mirror direction;

there are other directions, in which splashes in intensity are observed; with the increase of surface calibration degree (or with growth of its large-scale heterogeneity), the scattering pattern becomes more complicated.

The scattering is slightly dependent on the type of scattering surface, and there is a dependence of the scattering coefficient on the light-wave incidence angle. With increase of the incidence angle from 30° to 60°, the number of additional peaks decreases. Their most number is observed at $\theta_1 = 30°$. It is related to the influence of the height of irregularities of the surface on the scattering process.

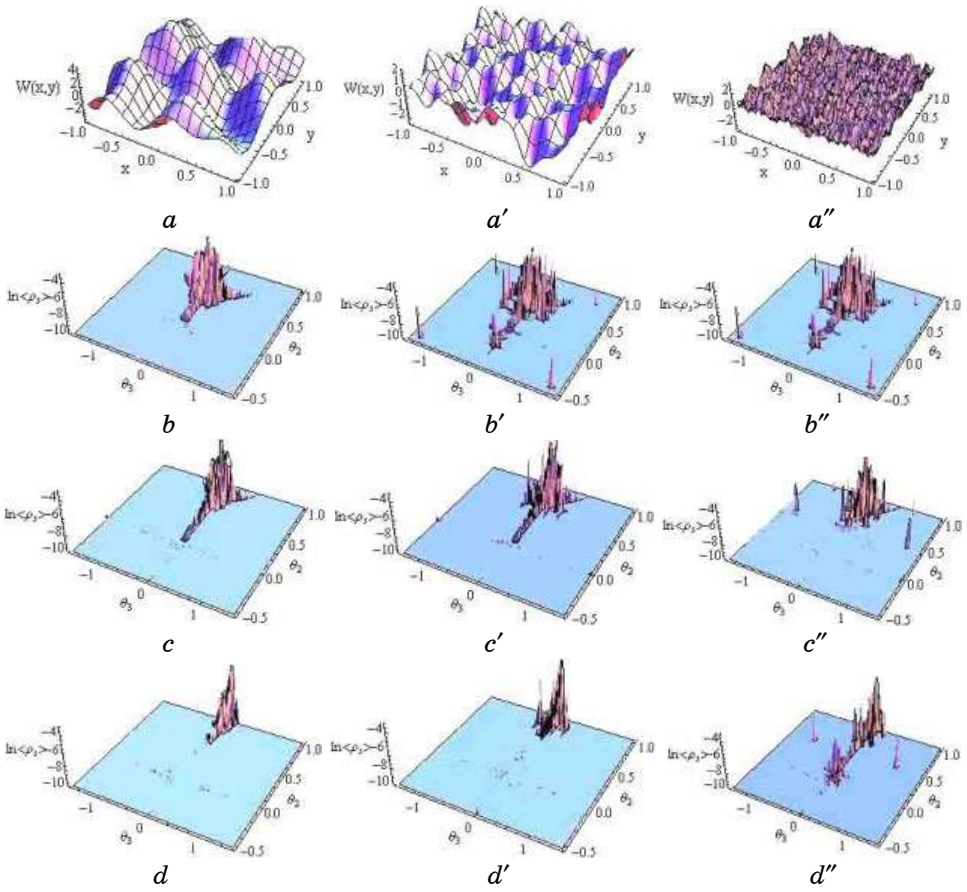

Fig. 2. Dependences of $\log\langle\rho_s\rangle$ on angles θ_1 and θ_3 for various types of fractal surfaces: *a*, *a′*, *a*—the samples of rough surfaces, for which the calculation of scattering indexes is produced; from top to bottom, the change of scattering index is routine for three angles of incidence: $\theta_1 = 30, 40, 60°$ (*a*–*d*, *a′*–*d′*, *a″*–*d″*) at $N = 5$, $M = 10$, $D = 2{,}9$, $q = 1{,}1$; $n = 2$, $M = 3$, $D = 2{,}5$, $q = 3$; $N = 5$, $M = 10$, $q = 3$, respectively.

The noted features of scattering are investigation of combination of chaotic state and self-similarity of the scattering-surface relief.

5. CONCLUSION

In this paper, the average coefficient of light scattering by surface fractal structures was calculated within the scope of Kirchhoff's method. A normalized band-limited Weierstrass function is presented for modelling of $2D$ fractal rough surfaces. On the basis of numerical calculations of average scattering coefficient, the scattering indicatrixes for various surfaces and incidence angles were calculated. The analysis of the indicatrixes leads us to the following conclusions: the scattering is symmetric about the incidence plane; with the increase of surface calibration degree, the scattering pattern becomes more complicated; the greatest intensity of the scattered wave is observed along the mirror direction; there are other directions, in which the intensity bursts are observed.

REFERENCES

1. T. G. Bifano, H. E. Fawcett, and P. A. Bierden, *Precis. Eng.*, **20**, No. 1: 53 (1997).
2. P. Wilkinson et al., *Wear*, **25**, No. 1: 47 (1997).
3. I. Sherrington and E. H. Smith, *Precis. Eng.*, **8**, No. 2: 79 (1986).
4. J. Kaneami and T. Hatazawa, *Wear*, **134**: 221 (1989).
5. K. Mitsui, *Precis. Eng.*, **8**, No. 40: 212 (1986).
6. J. W. Baumgart and H. Truckenbrodt, *Opt. Eng.*, **37**, No. 5: 1435 (1998).
7. C. J. Tay, S. L. Toh, H. M. Shang, and J. B. Zhang, *Appl. Opt.*, **34**, No. 13: 2324 (1995).
8. K. E. Peiponen and T. Tsuboi, *Opt. Laser Technol.*, **22**, No. 2: 127 (1990).
9. J. Q. Whitley, R. P. Kusy, M. J. Mayhew, and J. E. Buckthat, *Opt. Laser Technol.*, **19**, No. 4: 189 (1987).
10. M. Mitsui, A. Sakai, and O. Kizuka, *Opt. Eng.*, **27**, No. 6: 498 (1988).
11. T. V. Vorburger, E. Marx, and T. R. Lettieri, *Appl. Opt.*, **32**, No. 19: 3401 (1993).
12. C. J. Raymond, M. R. Murnane, S. S. H. Naqvi, and J. R. McNeil, *J. Vac. Sci. Technol. B*, **13**, No. 4: 1484 (1995).
13. D. J. Whitehouse, *Meas. Control*, **24**, No. 3: 37 (1991).
14. L. L. Madsen, J. F. J. Srgensen, K. Carneiro, and H. S. Nielsen, *Metrologia*, **30**: 513 (1994).
15. M. Stedman, *Proc. Int. Congr. X-Ray Optics and Microanalysis* (Manchester: IOP Publishing Ltd.: 1992), p. 347.
16. M. V. Berry and Z. V. Levis, *Proc. Royal Soc. London A*, **370**: 459 (1980).